

THE GENERATION OF HIGH TRAPPED FIELDS IN BULK (RE)BCO HIGH TEMPERATURE SUPERCONDUCTORS

D. A. Cardwell¹, W. K. Yeoh¹, S. K. Pathak¹, Y-H Shi¹, A. R. Dennis¹, N. Hari Babu², and K. Iida³

¹Superconductivity Group, Engineering Department, University of Cambridge, Cambridge, CB2 1PZ, UK

²Brunel Centre for Advanced Solidification Technology (BCAST), Brunel University, West London, UB8 3PH, UK

³The Leibniz Institute for Solid State and Materials Research Dresden (IFW)-Dresden, 01069 Dresden, Germany

ABSTRACT

Bulk, single grain RE-Ba-Cu-O [(RE)BCO, where RE represents a rare earth element or Y] high temperature superconductors (HTS) fabricated by top seeded melt growth (TSMG) have considerable potential for the generation of stable magnetic fields that are much larger than those produced by iron-based ferromagnetic materials (limited practically to less than 1.7 T). High trapped fields in bulk (RE)BCO are achieved by engineering effective flux pinning sites within the bulk microstructure that have similar dimensions to individual flux quanta, which exist in Type II superconductors. We report recent advances in the generation of flux pinning sites based on the engineering of RE₂BaCuO₅ (RE-211) and RE₂Ba₄CuMO_x (RE-2411) secondary phase inclusions in large grain (RE)BCO samples fabricated by a practical seeded melt growth process. Bulk samples of up to 26 mm in diameter have been fabricated by this process and shown to trap record magnetic flux densities in small samples at 77 K. The field-dependent critical current density in small sub-specimens and trapped field profile of single grain samples is reported.

KEYWORDS: Bulk superconductors, flux pinning, trapped magnetic field

INTRODUCTION

High temperature superconducting (HTS) bulk (RE)BCO (where RE = rare earth element such as Y, Gd, Sm Nd, etc.) single grains have the potential to trap large magnetic

fields compared to those produced by conventional permanent magnets [1-3]. Trapped field in bulk HTS can be improved by increasing the size of the single grain and/or the critical current density, J_c , of the bulk microstructure by the introduction of flux pinning centers. Non-superconducting second phase particles form particularly effective flux pinning centers if their size is comparable to approximately twice coherence length of the HTS material [4,5]. There are many methods of engineering the single grain microstructure to produce nano-size pinning centers, including reducing the particle size of the $\text{RE}_2\text{BaCuO}_5$ (RE-211) phase (the naturally-present second phase in (RE)BCO systems) [6-8], the addition of other (non RE-211) second phases [9,10] during processing and the creation of nano-size defects within the single grains by irradiating the sample with neutrons and/or heavy ions [11]. Of these, reducing the size of RE-211 and introducing new pinning centers are the most common and practical ways of improving J_c and, as a result, research worldwide has tended to focus on these techniques. Recently, $\text{Y}_2\text{Ba}_4\text{CuMO}_y$ [Y-2411(M)], where M = Nb, W, Ag, Bi, U, and Bi, has been identified and developed as an effective second phase composition for enhancing flux pinning in (RE)BCO single grain superconductors [12-15]. Nano-size particles of the non-superconducting Y-2411 phase have been found to be stable at elevated temperature during the growth of the superconducting $\text{REBa}_2\text{Cu}_3\text{O}_{7-d}$ phase, and their incorporation into the bulk microstructure has yielded J_c 's in bulk (RE)BCO superconductors as high as $1 \times 10^5 \text{ A/cm}^2$ in self-field at 77 K. Enriching the starting composition of the precursor powder with Y_2O_3 , rather than Y-211, has also been observed to improve J_c by reducing the Y-211 particle size. This paper summarizes the progress made towards enhancing J_c through either introducing finer RE-211 or nano-scale RE-2411 second phase inclusions to the bulk (RE)BCO microstructure and describes the development of a new, practical processing method to fabricate (LRE)BCO, where LRE = light rare earth, single grains in air that exhibit even higher trapped magnetic fields.

EXPERIMENTAL

Single grain Y-Ba-Cu-O (YBCO) and Gd-Ba-Cu-O (GdBCO) superconductors were prepared by a standard top seeded melt growth (TSMG) procedure [1]. Commercially available powders of the $\text{YBa}_2\text{Cu}_3\text{O}_y$ (Y-123) and $\text{GdBa}_2\text{Cu}_3\text{O}_y$ (Gd-123), with an average particle size of 1-3mm were used as the matrix precursors; Y_2O_3 (particle size 20-50 nm), Y_2BaCuO_5 (size 1-3mm) and $\text{RE}_2\text{Ba}_4\text{CuMO}_{12}$ phases were used as a source of second phase particles in the (RE)BCO composite. The $\text{RE}_2\text{Ba}_4\text{CuMO}_{12}$ phase [16] was synthesized as part of this study via solid state reaction. The following precursor compositions were then used to fabricate single grain bulk samples by TSMG:

- (i) 70 wt% Y-123 + 30 wt% Y-211 + 0.1 wt% Pt or 1 wt% CeO_2 ;
- (ii) 75wt% Y-123 + 25wt% Y_2O_3 + 1wt% CeO_2 ;
- (iii) Y-123 + 40 mol% Y-211 + x wt% $\text{Y}_2\text{Ba}_4\text{CuWO}_y$ + 10 wt% Ag_2O + 0.1 wt% Pt ;
x = 0, 2, 4, 6 and 8;
- (iv) 75 wt% Gd-123 + 25 wt% Y-211 + 0.1 wt% Pt + 10 wt% Ag_2O + 1 wt% BaO_2 ;
- (v) 75 wt% Gd-123 + 25 wt% Y-211 + 0.1 wt% Pt + 10 wt% Ag_2O + 2 wt% $\text{Gd}_2\text{Ba}_4\text{CuNbO}_{12}$ + 1 wt% BaO_2 .

Single grains with compositions (i) and (ii) were prepared specifically to investigate the influence of reduced Y_2BaCuO_5 particle size on the sample microstructure and its influence on J_c and trapped field.

Composition (iii) was prepared to study the presence of Ag on the formation and propagation of micro and macrocracks [17] and its influence on average bulk J_c of single grains containing $Y_2Ba_4CuNbO_y$ nano-inclusions.

Compositions (iv) and (v) were selected to investigate the development of a practical processing route [18] for the fabrication of GdBCO single grain superconductors in air. Excess BaO_2 was used in these samples to suppress formation of Gd/Ba solid solution, which reduces T_c [19].

Precursors with the above compositions were mixed thoroughly either with a milling machine incorporating an electrical grinder or manually with a mortar and pestle. The mixed powders were pressed uniaxially into pellets of various diameters (e.g. 16 mm, 20 mm, 26 mm and 32 mm). These pellets are placed on ZrO_2 rods to avoid direct contact with the Al_2O_3 ceramic substrates. One of two seed crystals was used independently to grow single grains to promote heterogeneous nucleation; a melt textured NdBCO seed and a generic NdBCO seed containing 1 wt% MgO [20]. In each case, the seed was placed on the top of the precursor pellet for both YBCO and GdBCO systems prior to the TSMG process. It is important to note that the size of each pressed pellet reduces significantly during melt processing due to shrinkage that takes place during melting of the precursor pellet (initial sizes of 16 mm, 20 mm, 26 mm and 32 mm produce final sample sizes of 13 mm, 16 mm, 20 mm and 26 mm, respectively). The temperature profile used for growing single grains varied significantly depending on the composition.

For the growth of YBCO single grains (compositions (i) and (ii)), pellets were heated to 1040 °C and held for 1 hour, cooled to 1003 °C at the rate of 120 °C /h and then slow cooled at a rate of 0.3 °C /h to 950 °C followed by fast cooling at a rate of 200 °C /h to room temperature.

A thermal gradient furnace was used to process compositions (iii), where the actual temperature in the vicinity of sample was ~ 20 °C higher than that of the set temperature. In this furnace, the precursor pellet and seed assembly was heated to 920 °C at 200 °C /h, 1000 °C at 300 °C /h followed by 2 h dwell, cooled to 940 °C at 28 °C /h, slowly cooled to 930 °C at 0.2 °C /h and then to 910 °C at 0.1 °C /h before cooling to room temperature at 200 °C /h. Unlike compositions (i) and (ii), slow cooling of 0.1 – 0.2 °C /h was necessary for this composition due to the reduced growth rate produced by the addition of Ag to the precursor.

Compositions (iv) and (v) were used to grow GdBCO single grains via a two step heating profile to suppress excessive liquid loss and also to suppress the formation of secondary grains. The pellets were heated to 1050 °C and held for 0.8 hour, cooled to 1020 °C at a rate of 120 °C /h and then cooled to 1000 °C at a rate of 0.4 °C /h. Finally, a slow cooling rate of 0.2 °C /h was employed to facilitate further growth of the single grain down to 980 °C. The actual temperature in the furnace was approximately the same as the set temperature during this process, and no external thermal gradient was imposed.

The melt processed YBCO single grains were annealed in flowing oxygen between 450 °C and 400 °C for 150 h in a tube furnace. An oxygen annealing temperature of between 440 °C and 360 °C for 300 h was used for the GdBCO single grain.

The smaller single grains (16 mm diameter) were cut into two halves along a diameter. One half was polished to expose the microstructure and the other was cut into small pieces ($1.0 \times 1.0 \times 0.5$ mm³) for measurement of its superconducting properties, such as T_c and J_c . A MPMS XL SQUID magnetometer was used to measure the magnetic moment as a function of temperature and the magnetic hysteresis loops of these specimens. The extended Bean model was used to calculate J_c from the latter. The larger single grains (20 mm and 26 mm diameter) were used for trapped field measurements. This involved cooling the samples initially using liquid nitrogen, followed by magnetization in an applied

field of 3 T. A Hall probe positioned 0.5 mm or 1.0 mm above the sample surface was scanned over the entire single grain after removal of the applied field.

RESULTS AND DISCUSSION

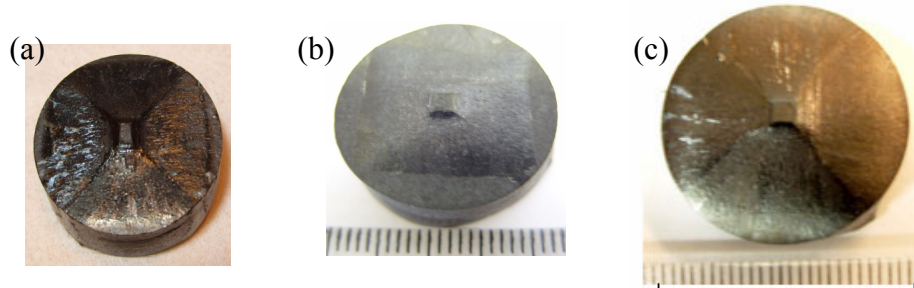


FIGURE 1. Photographs of (a) an YBCO single grain (20 mm dia) with composition (ii), (b) an YBCO single grain with composition (iii) for $x = 2$ and (c) a GdBCO single grain (26 mm dia) with composition (v).

The processing of YBCO single grain superconductors is now common across various research laboratories and industries. Figs. 1(a) and (b) show photographs of YBCO single grains fabricated from precursor pellets with compositions (ii) and (iii). However, the fabrication of GdBCO single grain superconductor is not as common as YBCO due to processing difficulties associated with lack of a suitable seed crystal and the formation of a Gd/Ba solid solution phase. These difficulties have been overcome recently by the development of a generic seed and the use of excess Ba to control solid solution formation during processing. Fig. 1(c) shows a photograph of a GdBCO melt-processed single grain fabricated from a precursor pellet of composition (v). Photographs of single grain samples of compositions (i) and (iv) are not shown in the figure. It can be seen in all cases that single grains with the *ab*-plane parallel to the top surface of the pellet have been grown without the formation of secondary grains.

Figures 2(a) and (b) compare the microstructures of YBCO single grains grown from precursor powders of composition Y-123/Y-211 and Y-123/Y₂O₃, respectively. A relatively homogenous distribution of Y-211 inclusions is present within the Y-123 matrix in both samples although the size of Y-211 particles in the sample processed from Y-123/Y₂O₃ precursors is generally smaller than those in the sample processed from the precursor containing Y-211. The average grain size is measured to be 1 and 1.5 mm for single grains fabricated from the Y-123/Y-211 and Y-123/Y₂O₃ precursor compositions [21]. The finer Y-211 particles present in Fig. 2(b) form as a direct consequence of the nano-size dimensions of the Y₂O₃ phase in the precursor powder. Y₂O₃ reacts with the Y-123 phase at 940 °C during the heating of precursor pellet, which leads to the formation of a Y-211 solid + CuO liquid phase [22]. This reaction leads directly to the formation of nano-sized Y-211 particles, which then coarsen during the cooling stage of the TSMG process. As a result, unlike in the case of enriching Y-123 with Y-211 phase particles, the final size of the Y-211 particles in the single grain grown from the Y-123/Y₂O₃ precursor depends strongly on the (nano-scale) size of the Y₂O₃ precursor particles. This suggests that the use of a fine-scale precursor powder is crucial to the refinement of Y-211 in the bulk matrix. J_c is known to vary in proportion to the ratio of the volume fraction (V_f/d) of second phase particles and their size d . The reduced particle size, therefore, increases V_f/d and potentially enhances flux pinning.

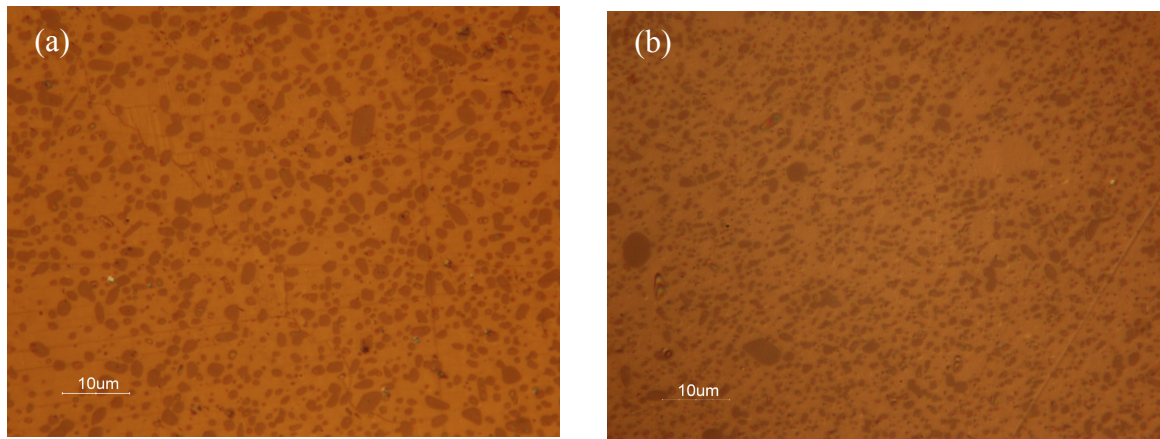


FIGURE 2. Optical micrographs of single grains fabricated from (a) Y-123/Y-211 and (b) Y-123/Y₂O₃ precursor compositions.

The enhancement in the average J_c for samples fabricated from precursors enriched with nano Y₂O₃ compared to Y-211 is shown in Fig. 3. It can be seen that the normalized J_c/J_{c0} data with applied field (inset to Fig. 3) for both samples are in relatively good agreement, except in the low field region (< 1 T). These results suggest that the pinning mechanism is predominantly the same in both samples (i.e. associated probably with the Y-123/Y-211 interface or with defects associated with the second phase particles), although the density and effectiveness of the flux pinning sites is improved substantially by using nano-size Y₂O₃, rather than Y-211, in the precursor powder.

A typical trapped field profile at 77 K of the sample containing Y₂O₃ of dimensions 20 x 20 x 9 mm³ with a maximum value of $B_T = 0.8$ T is shown in Fig. 4(a). This is the highest maximum value of B_T observed to date for an undoped YBCO sample of diameter 20 mm fabricated by TSMG. The variation of trapped field as a function of single grain radius

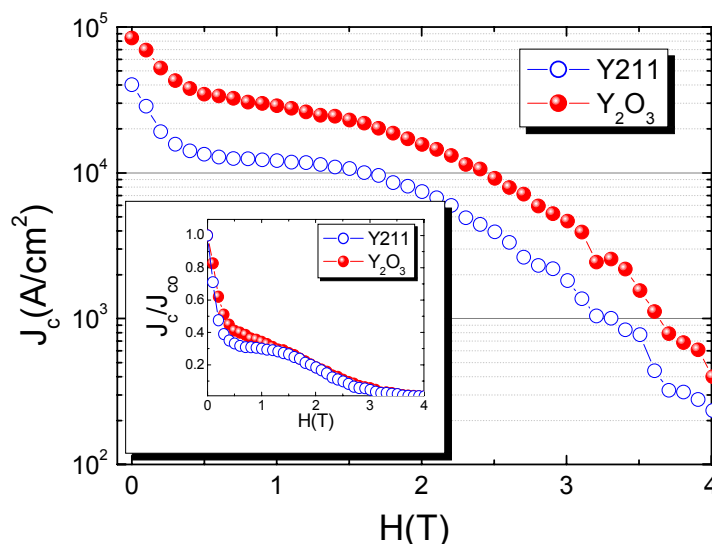


FIGURE 3. Average value of J_c calculated from magnetic hysteresis loops for samples at various locations within the bulk single grain as a function of field applied parallel to the c -axis at 77 K for samples fabricated from precursors containing Y-211 and Y₂O₃. The inset shows the normalized J_c for both samples.

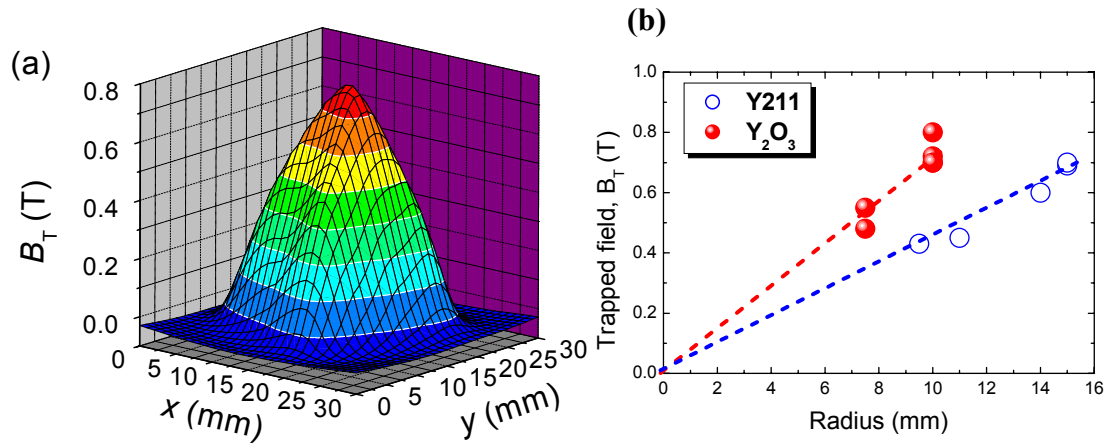


Figure 4. (a) Trapped field distribution at 77 K on the surface of YBCO single grain ($20 \times 20 \times 9 \text{ mm}^3$) fabricated from precursors enriched with nano-size Y_2O_3 . (b) Comparison of maximum trapped field, B_T , as a function of geometry for single grains fabricated from precursors containing Y-211 and Y_2O_3 . The dashed lines are linear fits to each dataset.

fabricated from precursors containing Y-211 and Y_2O_3 is shown in Fig. 4(b). The single grains fabricated in the present study from YBCO precursors containing Y-211 exhibit trapped fields that are comparable with those reported in the literature [23-25]. Fig. 4(b) indicates that the samples containing Y_2O_3 exhibit higher trapped fields and that trapped field increases more rapidly with increasing sample radius (i.e. measured by the gradient of linear fit to the data). This demonstrates clearly the potential of the addition of nano-scale Y_2O_3 to the precursor composition for generating significantly greater trapped fields than can be achieved in conventional YBCO single grains added with Y-211.

The addition of $(RE)_2Ba_4CuMO_y$ (RE-2411) to bulk (RE)BCO single grain superconductors has also been shown to enhance flux pinning of the composite. Unlike the RE-211 phase, however, the RE-2411 phases are chemically stable with the Ba-Cu-O liquid and have a negligible effect on the superconducting transition temperature, T_c , of the parent superconducting material [13]. As a result, their presence in bulk superconductors fabricated by TSMG has been demonstrated to contribute significantly to enhanced flux pinning [9,12-15]. Bulk J_c in these samples to date, however, has been limited

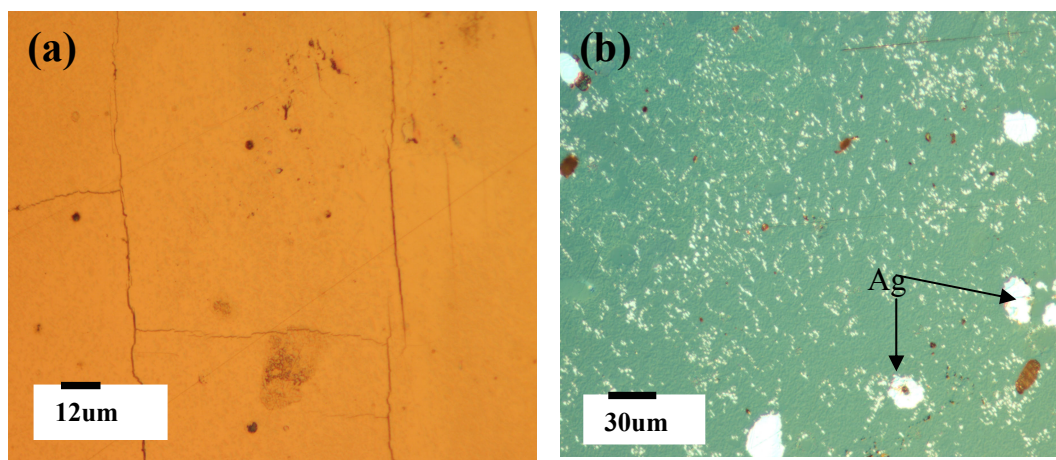


Figure 5. Optical micrograph of surface of polished single grain grown from composition (iii). (a) without addition of Ag_2O and (b) with addition of 10wt% Ag_2O to the precursors.

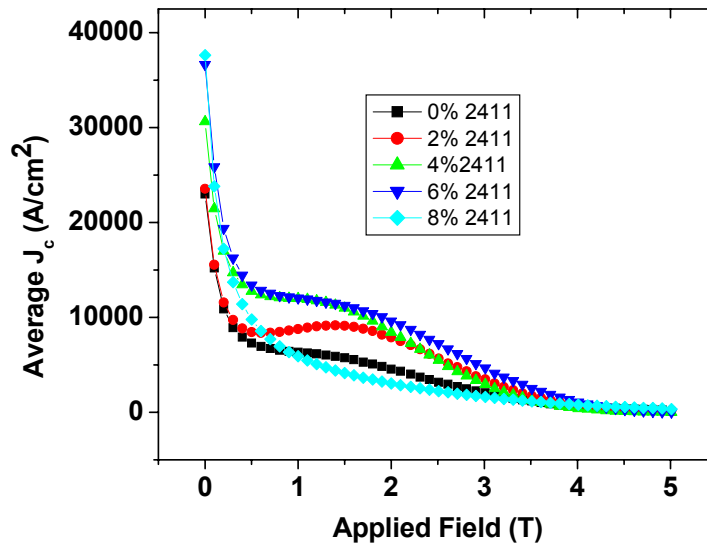


FIGURE 6. The average J_c of a large single grain containing various amounts of Y-2411.

significantly by the non-uniform distribution of second phase particles on a macroscopic scale and the intrinsically poor mechanical properties of the bulk superconducting matrix [26,27]. Macrocracks and cracks parallel to the c -axis, for example, limit severely the average bulk J_c of the single grain. Micro- and macrocracks also form from internal stresses during processing (the oxygenation process, in particular) and from stresses produced by thermal cycling between room and cryogenic temperatures. A large electromagnetic force acts on the superconductor during magnetization in samples in the critical state, which leads occasionally to catastrophic failure. It is therefore equally important to improve the microstructural properties of bulk superconductors if their field trapping capability is to be improved further [28-30]. Addition of Ag is known to reduce macrocracks and improves the fracture toughness of bulk superconductors [31]. The introduction of metallic Ag to single grain superconductors containing Y-2411 nano-scale inclusions has resulted in the formation of significantly fewer cracks than in samples fabricated without Ag, as shown in Fig. 5(a). Crack inhibition by the addition of Ag can be observed readily in the microstructures shown in Fig 5(b). The reduction in cracks is expected to prevent catastrophic fracture of samples that may otherwise fail due to high internal magnetic pressure.

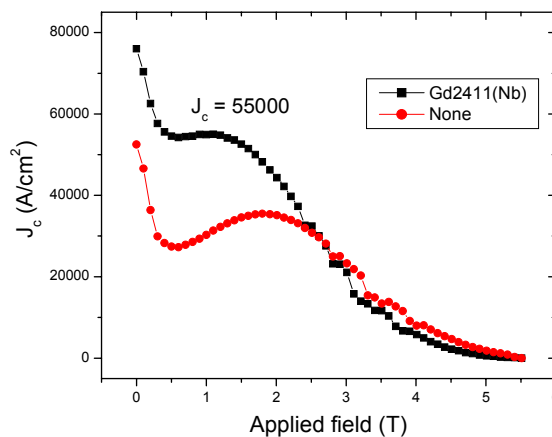


FIGURE 7. Comparison of measured J_c for GdBCO single grain with and without $Gd_2Ba_4CuNbO_y$ phase inclusions.

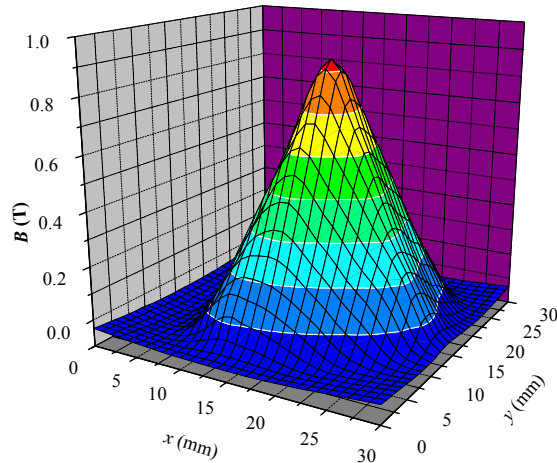


FIGURE 8. Trapped magnetic field for GdBCO single grain with $\text{Gd}_2\text{Ba}_4\text{CuNbO}_y$ phase inclusions at 77 K.

The J_c of 5 small pieces cut from the a and c growth sectors of single grains containing metallic Ag inclusions were calculated from measured hysteresis loops. Average J_c as a function of external field is shown in Fig. 6 for samples containing various amounts of Y-2411(Nb). Increasing J_c with increased concentration of Y-2411 phase inclusions in the Y-123 matrix suggests that the Y-2411 phase contributes to enhanced magnetic flux pinning. J_c under both self and applied external magnetic field is observed to increase in most cases in nano-composites due to increased magnetic flux pinning. The increased bulk J_c with increased Y-2411 content has been observed previously to contribute to increased trapped magnetic fields in single grain superconductors [32].

As in the case of the YBCO system, the influence of nano-scale inclusions on the critical current density of GdBCO single grains has been investigated by introducing Gd-2411 phase nano-scale inclusions into the Gd-123 phase matrix. Xu *et al* reported J_c as high as $84,500 \text{ A/cm}^2$ at zero field and 77 K for GdBCO containing $\text{Gd}_2\text{Ba}_4\text{MCuO}_8$ (where $M = \text{Mo}$) [33]. A trapped field for a single grain of diameter 24 mm processed in air was measured to be 0.56 T at 77 K for this sample. Unfortunately, bands of second phase particles formed inside the single grain during growth after adding Gd-2411 ($M = \text{Mo}$), which reduced its homogeneity. Fig. 7 shows comparison of J_c for the small samples cut from approximately the same distance from the seed location ($\sim 3\text{-}4$ mm away from the seed along a/b and c -axes) for single grains processed with and without Gd-2411(Nb). It can be seen that J_c of the sample containing Gd-2411(Nb) is higher over the whole range of applied field compared to the sample processed without Gd-2411(Nb). J_c as high as $5.5 \times 10^4 \text{ A/cm}^2$ was measured for this sample at 77 K and 1 T. This indicates that Gd-2411(Nb) has significant potential for flux pinning at higher operating fields. As a result of improved J_c , higher trapped magnetic fields have been recorded in this sample, as shown in Fig. 8. The trapped field profile exhibits good symmetry, which indicates a single grain. The peak value of trapped field in this sample is 0.9 T, which is one of the highest values for GdBCO single grains of size ~ 26 mm in diameter processed in air reported to date [34].

CONCLUSIONS

Flux pinning in single grain YBCO has been improved by engineering effective flux pinning sites within the bulk microstructure to sub-micron scale or nano-scale dimensions.

The Y-211 phase can be engineered on the sub-micron scale via the addition of nano-scale Y_2O_3 to the YBCO precursor powder prior to melt processing, which results in significantly improved trapped fields. The systematic increase in concentration of nano-scale $Y_2Ba_4CuNbO_x$ phase particles in large grain Y-Ba-Cu-O is observed to increase the average bulk J_c . GdBaCuO single grain nano-composites have been fabricated successfully in air to yield improved trapped magnetic fields but via a practical processing method. The development of a generic seed crystal that can be used for cold seeding for this system has enabled the fabrication of large single grain samples of up to 26 mm in diameter that shown to trap record magnetic flux densities in small samples (0.9 T for 26 mm diameter grain at 77 K).

REFERENCES

1. Cardwell, D. A. *Materials Science and Engineering B* **53** p.1 (1998)
2. Tomita M. and Murakami, M. *Nature* **421** p. 517(2003).
3. Litzkendorf, D.; Habisreuther, T.; Bierlich, J.; Surzhenko, O.; Zeisberger, M.;Kracunovska S.; Gawalek W. *Supercond. Sci. Technol.* **18**, p. S206 (2005)
4. Murakami, M.; Gotoh, S.; Koshizuka, N.; Tanaka, S.; Matsushita, T.; Kanube, S.; Kitazawa, K. *Cryogenics* **30**, p. 390 (1990).
5. Gomis, V., Pinol, S., Martinez, B., Fontcuberta, J. and Obradors, X. *Applied Superconductivity*, edited by H. C. Freyhardt (DGM, Oberursel), **1**, p.373 (1993).
6. Hari Babu, N., Shi, Y., Iida, K. and Cardwell D. A., *Applied Physics Letters* **87**, 202506 (2005).
7. Nariki, S., Seo, S. J. Sakai, N. and Murakami, M. *Supercond. Sci. Technol.* **13**, 778–784
8. Nariki S., Sakai N. and Murakami M., *Physica C*, **357-360** 811(2001).
9. Babu, N. H., Reddy E. S., Cardwell D. A., Campbell A. M., Tarrant C. D., and Schneider K. R., *Applied Physics letters*, **83** 4806 (2003).
10. Weinstein, R., Sawh, R. Ren, Y. and Parks, D. *Mater. Sci. Eng. B* **53** (1998) 38.
11. Civale L *et al Phys. Rev. Lett.* **67** 648 (1991).
12. Hari Babu, N., Shi, Y.-H., Iida K., Cardwell D. A., Haindl S., Eisterer M. and Weber H. W., *Physica C* **426-431** 520–526 (2005).
13. Hari Babu, N., Reddy E. S., Cardwell D. A. and Campbell A M., *Superconductor Science and Technology*, **16**, L44 (2003).
14. Hari Babu N., Iida K., Shi Y., Withnell T. D and Cardwell, D. A., *Superconductor Science and Technology* **19**, S461 (2006).
15. Cardwell D. A. and Hari Babu N., *Advances in Cryogenic Engineering*, **54**, p543-550 (2008).
16. Hari Babu, N., Iida, K., Briffa A., Shi Y., Matthews L., Cardwell, D. A., *IEEE Trans Applied Superconductivity*, **17**, 2953, (2007)
17. Pathak, S.K. Babu, N.H. Iida, K. Denis T., Matthews L., Strasik M., Cardwell, D.A. *Mat. Sci. Eng. B.* **151**, p40 (2008).
18. Hari Babu, N., Shi, Y-H., Iida, K. and Cardwell, D. A., *Nature Materials*, **4**, 476-480 (2005).
19. Shi, Y.-H., Hari Babu, N., Iida, K. and Cardwell, D. A.; *Journal of Materials Research*, **24**, p 10-18 (2009).
20. Shi, Y. Hari Babu N and Cardwell D. A., *Supercond. Sci and Tech* **18** L13 (2005).
21. Yeoh W. K., Pathak S. K., Shi Y-H, Dennis A R., Cardwell, D. A., Hari Babu N., Iida K. and Strasik M., *Superconductor Science and Technology* **22** 065011(2009)

22. Krabbes, G.; Schätzle, P.; Bieger, W.; Wiesner, U.; Söttver, G.; Wu, M.; Strasser, T.; Köhler, A.; Litzkendorf, D.; Fischer, K.; Görnert, P. *Physica C* **244**, 145 (1995)
23. Meng, R. L., Gao, L., Gautier-Picard, P., Ramirez, D., Sun, Y. Y. and Chu, C. W. *Physica C* **232** 337 (1994)
24. Fuchs, G.; Schätzle, P.; Krabbes, G.; Groß, S.; Verges, P.; Müller, K. H.; Fink, J.; Schultz, L. *Appl. Phys. Lett.* **76** 2108 (2000).
25. Takagi, A.; Miyamoto, T.; Ikuta H.; Mizutani, U. *Physica C* **412–414**, 586 (2004)
26. Ikuta H., Oka, T. Mizutani, U. buturi o yo (in Japanese), **68** 403 (1999).
27. Singh J. P. *et al*, *J. Appl. Phys.* **66** 1 (1989).
28. Ikuta H., Ikeda S., Mase A., Yanagi T., Yoshikawa M., Itoh Y., Oka T., Mizutani, U, *Applied Superconductivity*, Volume 6, Issues 2-5 109-117(1998).
29. Yen, F. White, K. W. *Japan. J. Appl. Phys.* **70** p. 4989(1991).
30. Ren Y., Weinstein, R. Liu, J., Sawh R.P. and Foster, C. *Physica C* **251** p. 15(1995).
31. Diko, P. Fuchs, G. Krabbes G. *Physica C* **363** pp. 60-66 (2001).
32. Pathak, S.K. Babu, N.H. Iida, K. Denis, A. R. Strasik, M. Cardwell, D.A. to be published.
33. Xu C., Hu, A. Sakai, N. Izumi, M. and Hirabayashi, I. *Supercond. Sci. Technol.*, **18** 1082 (2005).
34. Shi, Y. Hari Babu, N Iida, K Yeoh, W. Dennis A. R. and Cardwell, D. A. *Supercond. Sci. Technol.*, **22** 075025 (2009).